

# Effects of Interjet Spacing on Burning Multiple Sprays

K. Parvez\* and S. R. Gollahalli†

*The University of Oklahoma, Norman, Oklahoma, 73019*

In many large combustors multiple burners are employed to supply the required amount of fuel. Depending upon the design of multiple spray burners, several benefits such as reduction in flame length, control of heat-release pattern, and minimization of pollutant formation are possible. The physico-chemical processes, in terms of size, shape, atomization, evaporation, and burning characteristics of multiple spray flames, depend upon the mutual interaction of individual jets and the effects of surrounding airstream. In the present study three configurations, namely, 1-jet, 2-jets, and 3-jets arranged in a line, were used. Jet-A fuel was the liquid. Identical twin-fluid air-assist atomizers were employed. Four interjet spacings,  $a/d = 18.5, 24.7, 30.9$ , and  $37$ , where  $a$  was the distance between the jets and  $d$  was the atomizer exit diameter, were employed to study the effects of interjet spacing. Measurements included flame length, flame merging length, flame liftoff height, droplet size distribution, flame temperature, and major species concentrations. The transverse profiles in the near-nozzle region and the far-burner regions are presented. With an increase in interjet spacing, the amount of oxygen penetration through the space between the jets increases and leads to higher far-burner temperature, lower soot emission, and higher production of carbon monoxide and nitrogen oxides.

## Introduction

LIQUID fuel spray combustion, with all its complexities, is still a major source of energy for most of the combustion devices, such as boilers, gas turbines, ramjet engines, rocket combustors, diesel engines, and industrial furnaces. Most of the studies in the literature on liquid combustion deal with single drops, droplet arrays, or single spray jets. In many practical combustion devices, when large volume rates of fuel are required, it is advisable to split the inlet fuel stream into a number of single jets.

The interaction of individual jets with one another and with surrounding airflow influences their combustion characteristics. Several benefits such as reduction in flame length, smaller combustion chamber size, control of heat-release pattern, and minimization of pollutant formation can be achieved by employing multiple burner flames.

Several studies have been reported in the literature on the interaction of gas flames from multiple burners.<sup>1–4</sup> Chigier and Apak<sup>1</sup> studied the interaction of multiple turbulent natural gas diffusion flames with different degrees of swirl and burner separation distance. They documented temperature and concentration profiles, flame stability, and flame length and concluded that for flames separated by more than two exit diameters there was no significant interaction. They also found that the interaction effects were accentuated with an increase in swirl number. Menon and Gollahalli<sup>2,3</sup> studied the flame structure and pollutant emissions of propane gas jets separated by various distances both in quiescent conditions and in a crossflow. They found significant coupling effects of the jet-crossflow momentum flux ratio on the interaction of multiple burner flames. Recently, Tillman et al.<sup>4</sup> have studied the interaction of planar gas jet flames and found that blowoff velocity increased for multiple burners. However, the studies on burning sprays from multiple injectors are severely limited. Although the aforementioned benefits can be expected in the case of burning sprays also, depending upon the relative spacing and orientation of injectors forming these sprays some undesirable effects such as an enhancement of soot formation can occur. This paper presents an experimental study of the effects of interjet spacing of three liquid sprays on their combustion character-

istics including the distribution of droplet size and velocity, radiation emission, temperature profiles, species concentration profiles, emission indices of pollutant species, and soot concentration profiles. The general appearance of the flame, in terms of the flame liftoff height, flame length, and flame merging length has also been investigated.

## Experimental Apparatus and Procedure

Experiments were conducted in a laboratory scale combustion chamber. The chamber was mounted vertically and was constructed of 6-mm-thick steel plates. The interior of the chamber was 164 cm tall and 76-cm square in cross section. High-temperature Pyrex glass sheets (dimension  $30 \times 140$  cm) were fixed on three of the four walls of the chamber to provide an optical access for flame visualization. The fourth wall of the chamber was replaced by an aluminum plate, which had a vertical slot so that the thermocouple and gas sampling probe could be inserted into the chamber for measurements. A cooling fan was mounted on top of each window to keep Pyrex glass sheets cool and prevent them from cracking caused by high temperature. One of the chamber walls was provided with a small access door for igniting the fuel jet when the chamber was closed. The bottom plate of the chamber had two horizontal 10-cm-long and 0.5-cm-wide slots to accommodate the three atomizers and to facilitate variations in interjet spacing and injection angles by sliding and locking the atomizers in the slots at the appropriate locations.

Three identical external-mixing twin-fluid (air-assist) injectors were used in the present study. The injector exit diameter  $d$  was 1.62 mm. Two concentric jets, the liquid jet being the inner, emerged at the nozzle exit. The high-velocity airstream impinged on the liquid at or outside the liquid discharge orifice resulting in the atomization of liquid. The injectors were connected to the fuel and primary (atomizing) air lines and mounted on the base plate of the chamber producing spray jets in the vertically upward direction.

Jet-A fuel was used in the present study. The fuel was supplied from a tank under the pressure of bottled nitrogen to the atomizers through needle valves and rotameters and a  $15\text{-}\mu\text{m}$ -pore liquid fuel filter. Primary air was supplied by a vane-type rotary compressor and was metered using a separate rotameter for each atomizer. The top of the combustion chamber was attached to an exhaust duct of a 32-cm-square cross section. An axial exhaust fan was installed in the exhaust duct for creating an induced draft. A manually operated damper was used to control the rate of suction of the exhaust.

Several instruments were used to record the following data: 1) radiation emission, 2) visible total flame length, 3) merging height of flames, 4) liftoff height of individual sprays, 5) droplet size, 6) droplet velocities, 7) species concentrations, 8) emission indices

Received 8 July 1999; revision received 6 January 2000; accepted for publication 6 January 2000. Copyright © 2000 by K. Parvez and S. R. Gollahalli. Published by the American Institute of Aeronautics and Astronautics, Inc., with permission.

\*Research Assistant, Combustion and Flame Dynamics Laboratory.

†Lesch Centennial Professor, Combustion and Flame Dynamics Laboratory. Associate Fellow AIAA.

of pollutant species, 9) temperature profiles, and 10) soot concentration. Radiative heat emission of the flame was measured with a broadband wide-view-angle radiometer. To minimize the effects of solid angle variation and to satisfy the inverse square law, the distance between the radiometer and the flame exceeded 1.5 times the length of the flame. The readings were corrected to account for the thermal radiation from the chamber walls in the field of view.

Simultaneous measurements of droplet size and velocity were made using a phase Doppler particle analyzer (PDPA). A 10-mW helium-neon laser with an output beam diameter of 0.68 mm was employed in the transmitter. The receiver of PDPA consisted of a lens system for light collection through a 100-μm-wide slit. The focal length of the transmitter output lens was set to 495 mm and that of collimating lens was set to 300 mm with the PDPA software. The instrument was used in the forward scatter mode at 30-deg off-axis angle. The transmitter and the receiver were mounted on two rigid traverse mechanisms, Flame temperature was measured with a Platinum-Platinum/13% Rhodium (type R) thermocouple constructed locally using fine wires of 0.1 mm diam to form a bead of diameter 0.22 mm. A thin silica layer was applied on the bead to minimize catalytic effects. A microcomputer was used for data acquisition at 10 Hz. The readings were averaged over 180 samples and corrected for radiation and conduction losses.

The concentrations of nitric oxide (NO), carbon-dioxide (CO<sub>2</sub>), carbon-monoxide, and oxygen (O<sub>2</sub>) were measured in the flame. The sampling system consisted of an uncooled quartz probe (1.5 mm inner diameter) mounted on a precise traversing assembly, a moisture condenser, two glass wool and paper cartridge filters to trap particles, Teflon lines, and analyzers. A rotameter was also employed in the line to allow for isokinetic sampling. The following analytical instruments were employed: 1) a polarographic catalyst type oxygen analyzer, 2) nondispersive infrared CO and CO<sub>2</sub> analyzers, and 3) a chemiluminescent NO/NO<sub>x</sub> analyzer. The emission indices of CO, NO, and NO<sub>x</sub> were determined from the concentrations measured with the same instruments in the flame exhaust using a trapezoidal collector.

Soot concentration was measured using a standard light-scattering and extinction technique. Soot volume fraction was calculated with the laser-beam attenuation method. A 0.95-mW helium-neon optical laser was used as a radiation source. The laser was directed through the flame from one side of the chamber, and it was detected from the other side by a detector, which was equipped with silicon sensors. The output of the detector was fed to a microprocessor-driven power meter, which displayed the output in digital form. At each point in the flame, three measurements were made: 1) laser input intensity without flame  $I_{in}$ , 2) laser output intensity with flame  $I_{f+o}$ , and 3) only intensity of the flame  $I_f$ .

A camcorder was employed to measure the flame liftoff height, flame length, and flame merging length. The flame length  $L_f$  was taken as the distance between the nozzle exit and the end of the contiguous portion of the flame visible in the video picture. Similarly, merging length  $L_m$  was considered as the distance from the nozzle exit to the lowest point at which the flames appear to touch each other in the video picture. The flame liftoff height was taken as the distance from the jet exit to the lowest point at which the visible flame was stabilized. Figure 1 defines the flame length, flame merging length, and flame liftoff height. Tables 1 and 2 show the experimental conditions and the fuel properties.

In the present study a standard statistical test (Student's t-test-Schenck)<sup>5</sup> was employed for the uncertainty analysis. The uncertainties in results are presented in Table 3.

Results and Discussion

Flame Length, Flame Merging Length, and Flame Liftoff Height

The effects of interjet spacing  $a/d$  on flame length are presented in Fig. 2 for different number of jets  $n$ . Flame length increases with a decrease in interjet spacing  $a/d$ . This increase in flame length with the decrease in interjet spacing can be explained as follows: in spray combustion, fuel droplets evaporate, mix with air, and burn. With a decrease in interjet spacing, more fuel vapors accumulate in a

Table 1 Properties of liquid fuel

Property	Value
Gravity-° API	43.00
Reid vapor pressure kPa @ 298 K	1.38
Freeze point, K	227.00
Viscosity@ 280 K cs	9.40
Sulfur, wt. %	0.60
Aromatic, wt. %	17.20
Heating value, net MJ/kg	43.90

Table 2 Experimental conditions

Parameter	Value
Fuel flow rate through each injector	$3.84 \times 10^{-4}$ kg/s
Fuel tank pressure	0.2 MPa
Atomizing airflow rate through each injector	$1.34 \times 10^{-4}$ kg/s
Supply pressure atomizing air	0.17 MPa
Atomizing air temperature	298 K
Ambient pressure	$28.7 \pm 1.5$ cm Hg
Ambient temperature	$295 \pm 3$ K
Relative humidity	$65 \pm 5\%$

Table 3 Estimated values of uncertainty<sup>a</sup>

Measurement	Symbol	Exp. uncertainty % of mean value
Flame temperature	$T$	0.88
Concentration of CO	$X_{CO}$	3.2
Concentration of CO <sub>2</sub>	$X_{CO_2}$	3.0
Concentration of NO	$X_{NO}$	3.5
Concentration of O <sub>2</sub>	$X_{O_2}$	3.6
Flame length	$L_f$	2.7
Flame merging length	$L_m$	7.5
Flame liftoff height	$L_l$	9.2
Droplet diameter	$D_{(10)}$	4.7

<sup>a</sup>At 95% confidence value with t-distribution.

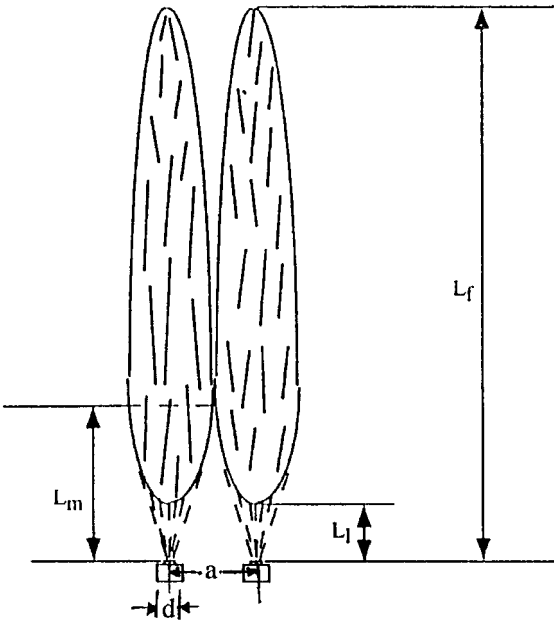


Fig. 1 Definitions of flame length  $L_f$ , merging height  $L_m$ , and liftoff height  $L_l$ ;  $d$  = atomizer exit diameter,  $a$  = distance between jets,  $n$  = number of jets.

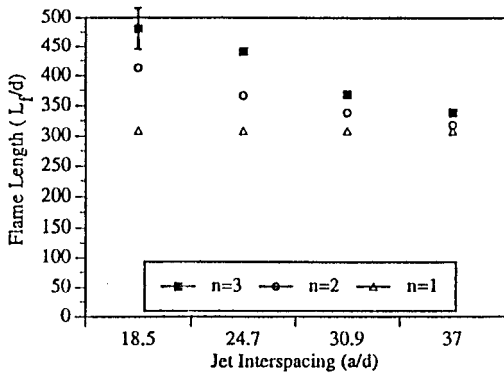


Fig. 2 Effect of interjet spacing on visible flame length.

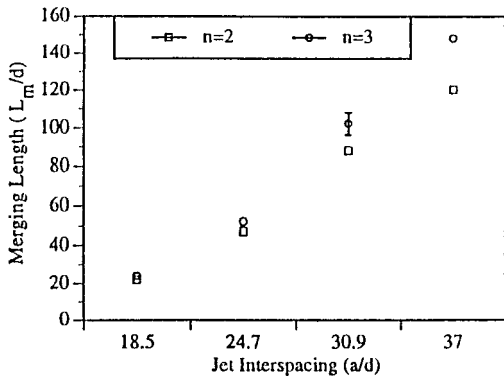


Fig. 3 Effect of interjet spacing on merging length.

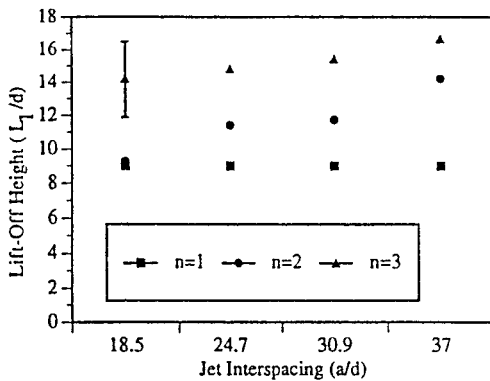


Fig. 4 Effect of interjet spacing on liftoff height.

smaller volume. Fuel vapors try to reach air by diffusing radially. If air is already consumed at the flame edge, the vapors then travel axially to access air at a downstream location. This process continues until all vapors are consumed resulting in an increase in the flame length.

Figure 3 shows the effects of interjet spacing on flame merging length. It is apparent that the merging length increases with an increase in interjet spacing. This is attributed mainly to geometrical arrangements and the effects of physico-chemical process. The linear increase in the width of turbulent axisymmetric jets with axial distance results in an increase in merging height as the interjet spacing is increased. Because the central jet is exposed to the similar conditions on both sides, the merging length is same on either side.

The effects of interjet spacing on flame liftoff height of the central jet are shown in Fig. 4. The liftoff height of the outer jets does not change significantly with a change in interjet spacing. However, the liftoff height of the central jet is slightly larger than those of the outer jets. It is caused by the fact that three sides of each outer jet are exposed to still atmosphere, whereas only two sides of the central jet are exposed to quiescent air environment. Therefore, the central

jet is subjected to lesser shear than the outer jets. Hence, the axial component of the gas velocity at the flame base remains higher in the central jet. Furthermore, the lower availability of oxygen in the interspace reduces the flame velocity of propagation. A combination of these two effects results in a higher liftoff distance for the central jet. A decrease in interjet spacing results in more fuel vapors between the jets, and the stoichiometric contour moves upstream resulting in a lower liftoff height.

The results of the study are significant in combustor design, especially where space considerations are paramount, such as aircraft combustion chambers. The diameter of a combustor is restricted by the overall aircraft engine diameter, and its length is subjected to the space available between compressor and turbine. For a given fuel the interjet spacing can be adjusted according to the restricted requirements. If longer axial distance is available and a slim engine is required, then decrease in separation distance between the jets will be helpful. Of course, there may be some penalty in terms of pollution formation. On the other hand, if the engine has to be larger in diameter and shorter in length, an increase in interjet spacing is beneficial for the given fuel flow rate.

### Droplet-Size Distribution

The effects of interjet spacing on spray characteristics are examined by measuring the radial profiles of droplet mean diameter (SMD) and mean velocity with the PDPA at various axial positions.<sup>6</sup> Figure 5 shows the typical effects of interjet spacing on droplet-size distributions. The results show that the jets behave independently of each other, indicating atomization characteristics are not affected by the interaction effects caused by multiple jets. These findings are in close agreement with those of Krothapalli et al.<sup>7</sup> and Marsters.<sup>8</sup> They have reported that in multiple jet configurations in the near-nozzle region jets behave as though they are single. Droplet diameter peaks occur at the individual jet boundaries. A gradual increase in the mean droplet diameter in radial direction for each individual jet is apparent, which is attributed to the characteristics of the type of atomizer. Similar results have been reported by Yule et al.<sup>9</sup> and Presser et al.<sup>10</sup> for similar atomizers. It is also evident that SMD

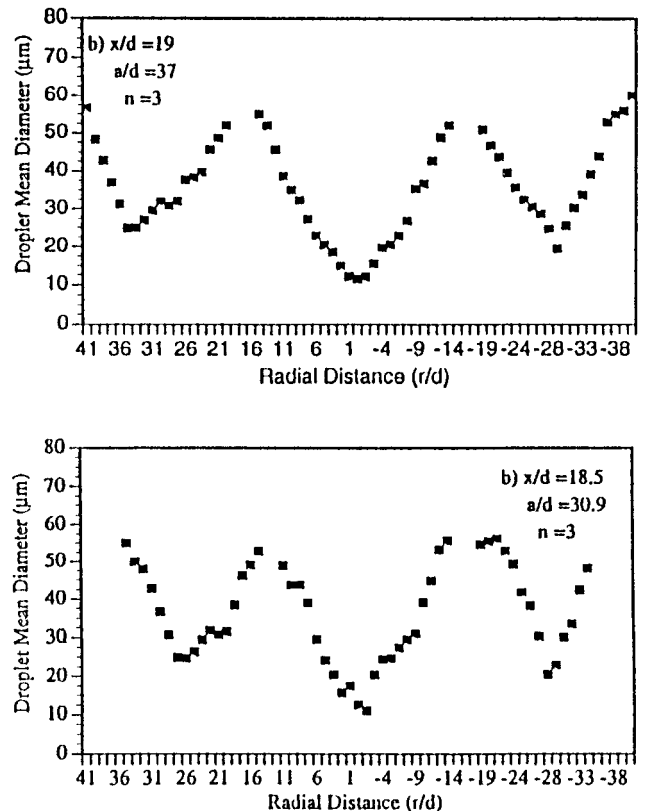


Fig. 5 Effect of interjet spacing on drop-size distribution.

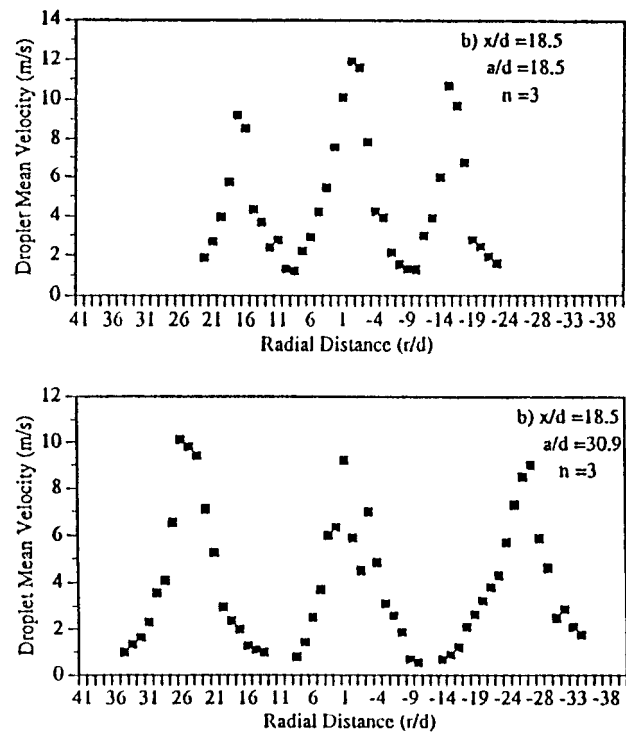


Fig. 6 Effects of interjet spacing on drop velocity distribution.

increases along the axial direction. This increase in diameter with downstream direction is caused by vaporization or dispersion of smaller droplets. As the evaporation proceeds, smaller drops disappear, resulting in an increase in the percentage of larger drops. These results are in good agreement with those of Dodge and Moses.<sup>6</sup>

Droplet Velocity Distribution

The effects of interjet spacing on droplet velocity profiles are shown in Fig. 6. Droplet velocity gradually decreases along the axial direction as well as along the radial direction. This behavior is in accordance with the well-established jet behavior, i.e., the velocity is maximum at the centerline of the jet and decreases along the radial and axial directions. Furthermore, droplets of smaller diameter, which are more numerous near the flame axis, are subjected to lesser drag force than their counterparts of larger diameter at the flame edges. This, to some extent, contributes to the present velocity pattern. The measurements at several other interjet spacings reported in Parvez<sup>11</sup> show that the droplet mean velocity decreases with the increase in interjet spacing. With an increase in interjet spacing, fuel vapor/atomizing air flux decreases in the area covered by the jets, which leads to a decrease in droplet mean velocity.

Radiative Fraction of Heat Release

A radiometer was used to measure the total radiative heat flux emitted by the flames. Radiative fraction of heat release was calculated assuming complete combustion of the fuel, which is reasonable, at least for heat-release calculations, because no free smoke was seen from the flames in the present experiments. Figure 7 shows the effects of interjet spacing on the radiative fraction of heat release *F*. The radiative fraction of heat release decreases slightly with the increase in interjet spacing. Radiation emission depends on both temperature level and emissivity of flames. The emissivity in hydrocarbon diffusion flames, in turn, depends strongly on the burning soot concentration and flame volume. In multiple jet flames, as the jets are brought together, the insufficiency of oxygen leads to more soot formation as discussed later. As the interjet spacing increases, less soot concentration is found in the far-burner region, and the local flame gas temperature increases as discussed later in the paper. These counteracting effects lead to only a slight decrease in the radiative fraction of heat release.

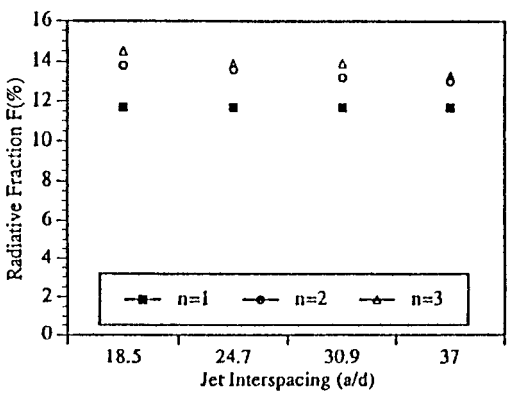


Fig. 7 Effects of interjet spacing on radiative fraction of heat release.

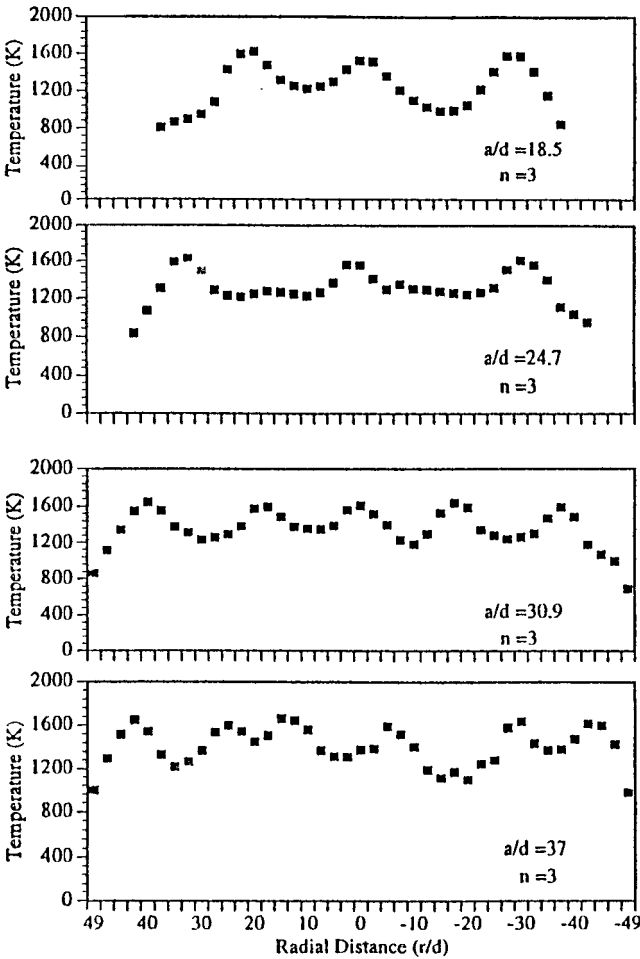


Fig. 8 Effects of interjet spacing on the transverse temperature profiles in the near-burner region ( $x/L_f = 0.25$ ).

Temperature Profiles

Radial temperature profiles are measured in three flame regions: near-nozzle region, midflame region, and far-nozzle region. Figures 8 and 9 present the effects of interjet spacing on temperature profiles in the near- and far-burner regions. The midflame profiles are available in Parvez.<sup>11</sup> To avoid errors caused by impingement of numerous liquid drops on the thermocouple bead, all measurements, in the near-nozzle region, were made at or near 150 mm from the nozzle exit. In single-jet liquid fuel sprays the maximum temperature occurs at the boundaries, and the minimum temperature occurs on the axis of the jet. In a 3-jet configuration, at small interjet spacing when flames merge four temperature peaks appear. Two of these peaks correspond to the locations of the flame interfaces when the flames

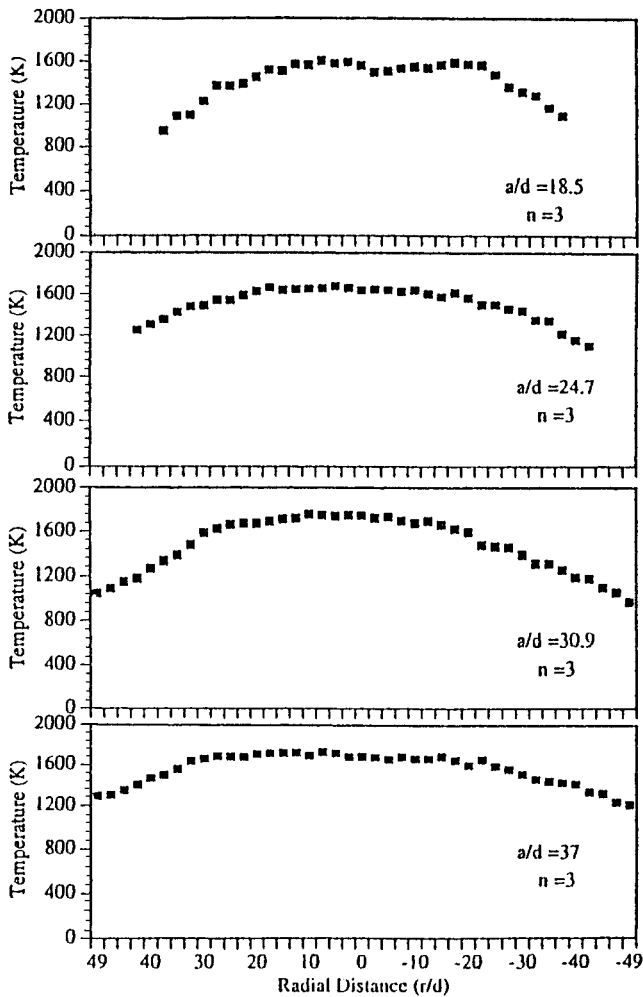


Fig. 9 Effects of interjet spacing on the transverse temperature profiles in the far-burner region ( $x/L_f = 0.67$ ).

merge, and two others correspond to the outer edges of the outer jet flames. At larger interspacings where flames do not merge, six peaks appear, two peaks corresponding to the edges of each of the three flames.

Figure 8 shows the temperature profiles in the near-nozzle region. This figure indicates that, at relatively smaller interjet spacings, the mixing effects are stronger than those at larger interjet spacings. The upper two profiles of Fig. 8, which correspond to  $a/d = 18.5$  and 24.7, have three temperature peaks instead of four. Six temperature peaks are quite apparent in case of the largest interjet spacing ( $a/d = 37$ ). These results indicate that mixing level decreases with the increase in interjet spacing. Temperatures at the edges of the central jet are slightly lower than those at the edges of the outer flames in cases of relatively smaller interjet spacings. The peak value of temperature is not significantly affected by the value of interjet spacing.

Temperature profiles in the far-nozzle region are shown in Fig. 9. Almost all of the temperature profiles appear without multiple peaks. This is because of the fact that soot combustion, which depends upon chemical kinetics and not diffusion-controlled interface combustion, dominates in the far-nozzle region. Furthermore, from Figs. 8 and 9 the peak values of temperature profiles, in the far-nozzle region, increase slightly with the increase in interjet spacing. The central jet temperature in a multijet configuration is affected by two factors: the oxygen availability, a reduction of which lowers the oxidation rates and leads to a lower peak temperature; radiation shielding, which lowers the heat loss rate and hence increases the peak temperature. The fact that the peak temperature is lower at smaller interjet spacings indicates that the former effect is more dominant.

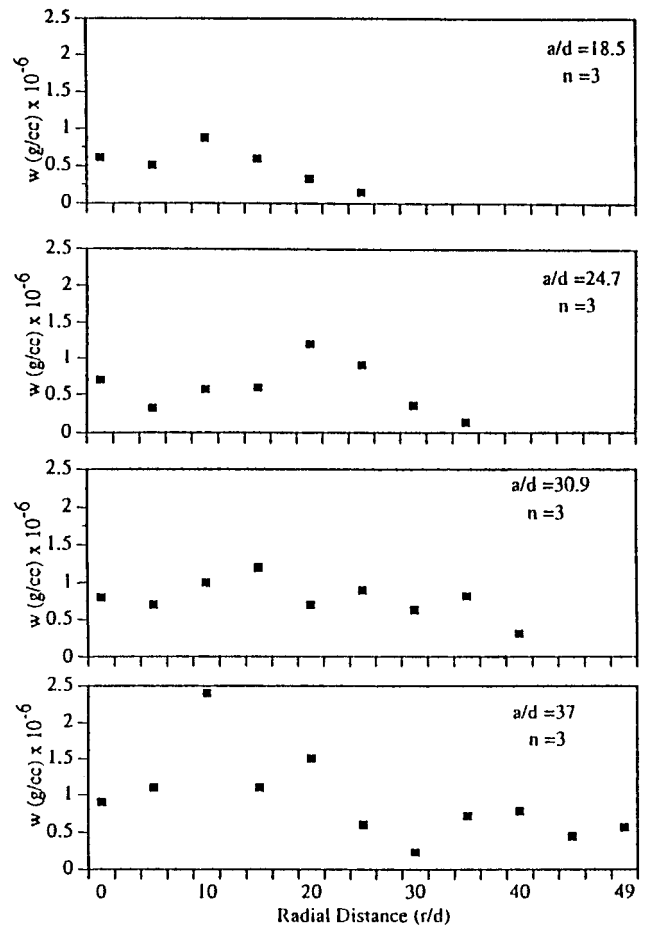


Fig. 10 Effects of interjet spacing on soot concentration profiles in the near-burner region ( $x/L_f = 0.25$ ).

#### Soot Concentration

From the laser attenuation measurements soot volume fraction was calculated.<sup>11</sup> Measurements were conducted to generate radial soot concentration profiles for the three flame regions. The effects of interjet spacing on soot concentration at  $x/L_f = 0.25$  and 0.67 are shown in Figs. 10 and 11. At those axial locations most of the droplets were evaporated and did not affect the attenuation measurements significantly. The observation has been made that soot concentration is low where the flame temperature is high and vice versa.

Flame temperature affects soot formation in two ways: 1) insignificant changes in the peak flame temperature in the near nozzle does not change fuel pyrolysis rate and the formation of soot particles, and 2) on the other hand, higher temperatures in the far-burner region results in a faster burning of soot particles. Therefore, the peak value of soot concentration in the near-nozzle region does not change markedly, whereas it decreases in the far-nozzle region with an increase in interjet spacing. The results in Ref. 2 also reveal that soot concentration, in case of the smaller interjet spacing ( $a/d = 18.5$ ), increases with an increase in the axial distance, reaches maximum value in the midflame region, and then decreases in the far-nozzle region. Similar findings have been reported by Prado et al.<sup>12</sup>

#### Emission Indices of CO, NO, and NO<sub>x</sub>

Emission indices for CO, NO, and NO<sub>x</sub> are determined for all flames by measuring their concentrations in the exhaust gases, which are channeled through a trapezoidal collector. Emission indices are presented in terms of the mass rate of emission of a species per joule of useful energy in the units of ng/J.

Figures 12–14 present the effects of interjet spacing on the emission indices of CO, NO, and NO<sub>x</sub>. Figure 12 shows the effects of interjet spacing on the emission index of carbon monoxide. It appears

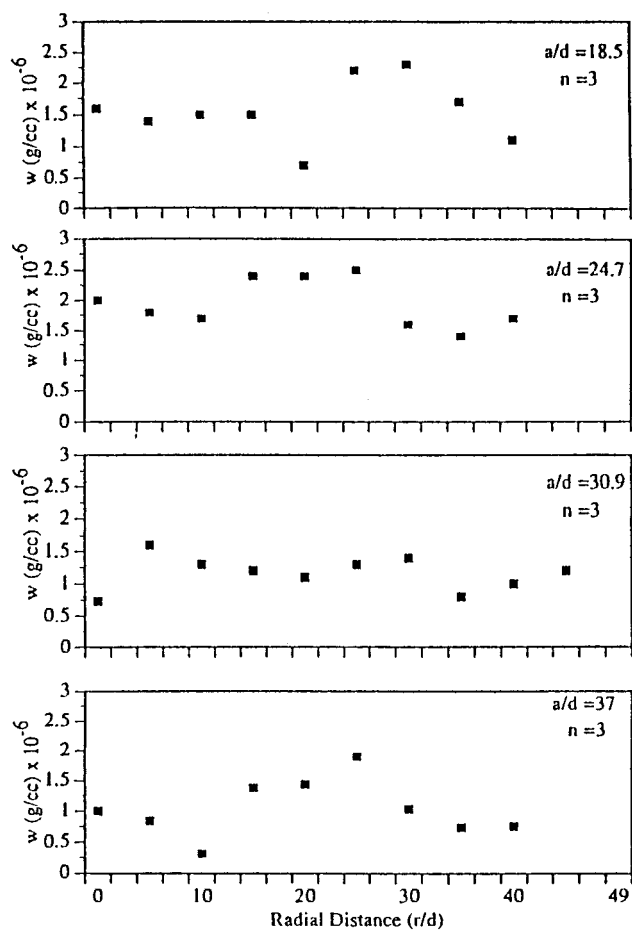


Fig. 11 Effects of interjet spacing on soot concentration profiles in the far-burner region ( $x/L_f = 0.67$ ).

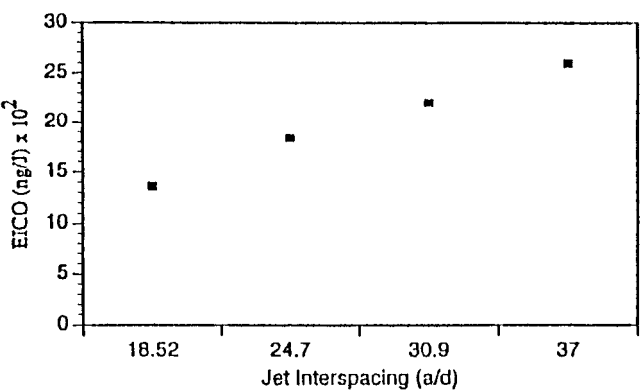


Fig. 12 Effect of interjet spacing on the emission index of carbon monoxide.

that the emission index of carbon monoxide increases with the increase in interjet spacing. Oxygen concentration in the far-nozzle region increases with the increase in interjet spacing and enhances the oxidation rate of soot to CO; however, the oxidation rate of CO to CO<sub>2</sub> is slow, which leads to an accumulation of CO.

The variation in the emission index of nitric oxide with interjet spacing is shown in Fig. 13. The emission index of nitric oxide increases with the increase in interjet spacing. This is attributed to the fact that the reactions in midflame and far-nozzle approach stoichiometric conditions with the increase in interjet spacing and hence increases the NO emission index. Similar results, in case of NO<sub>x</sub> emission, can be seen in Fig. 14. It is reported by Gupta et al.<sup>13</sup> that the ratio of NO<sub>x</sub> to NO emission indices is approximately two. The results of the present study also indicate that the ratio of NO<sub>x</sub>

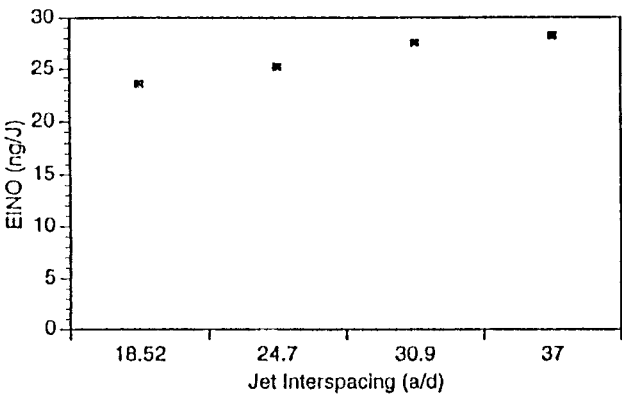


Fig. 13 Effect of interjet spacing on the emission index of nitric oxide.

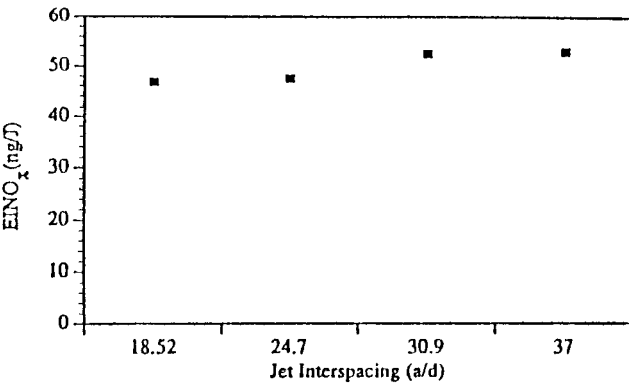


Fig. 14 Effect of interjet spacing on the emission index of nitrogen oxides.

to NO emission is two. This shows that although the amount of NO formed increases with the increase in interjet spacing the relative amount of NO<sub>2</sub>, which is oxidized to form NO<sub>x</sub>, remains at a constant ratio to the amount of NO<sub>x</sub> formed. This suggests that NO<sub>x</sub> formed is not directly dependent on the interjet spacing, but rather on the amount of NO formed.

Conclusions

With an increase in interjet spacing, the amount of oxygen penetration through the space between the jets increases, which leads to higher temperature, lower carbon monoxide formation, higher NO production, higher carbon dioxide, and lower soot formation. Furthermore, an increase in jet interspacing leads to a decrease in flame length, an increase in merging length and liftoff height, and a small decrease in radiative fraction of heat release. Emission indices of CO, NO, and NO<sub>x</sub> increase with an increase in interjet spacing. There are no indications of interaction effects, because of all but one interjet spacing, on atomization process in the near-nozzle region. Atomization characteristics are affected at small interjet spacings, namely,  $a/d = 18.5$ .

References

<sup>1</sup>Chigier, N., and Apak, G., "Interaction of Multiple Turbulent Diffusion Flames," *Combustion Science and Technology*, Vol. 10, No. 1-3, 1975, pp. 219-231.

<sup>2</sup>Menon, R., and Gollahalli, S. R., "Multiple Jet Gas Flames in Still Air," *Heat Transfer and Fire in Combustion Systems*, HTD-Vol. 45, American Society of Mechanical Engineers, New York, 1985, pp. 127-136.

<sup>3</sup>Menon, R., and Gollahalli, S. R., "Combustion Characteristics of Interacting Multiple Jets in Cross-Flow," *Combustion Science and Technology*, Vol. 60, No. 4-6, 1988, pp. 375-389.

<sup>4</sup>Tillman, S. T., Annamalai, K., and Caton, J., "Lift-off and Blow-off Characteristics of Laminar Nonpremixed Planar Jets," *Proceedings of the ASME Heat Transfer Division*, HTD-Vol. 352, American Society of Mechanical Engineers, New York, 1997, pp. 101-108.

<sup>5</sup>Schenck, H., *Theories of Engineering Experimentation*, Hemisphere, Washington, DC, 1979, pp. 272-275.

<sup>6</sup>Dodge, L. G., and Moses, C. A., "Diagnostics for Fuel Sprays as Applied to Emulsified Fuels," *Twentieth International Symposium on Combustion*, Combustion Inst., Pittsburgh, PA, 1984, pp. 1239-1247.

<sup>7</sup>Krothapalli, A., Baganoff, D., and Karamcheti, K., "Development and Structure of Rectangular Jets in Multiple Jet Configuration," *AIAA Journal*, Vol. 18, No. 8, 1980, pp. 945-950.

<sup>8</sup>Marsters, F. G., "Interaction of Two Plane Parallel Jets," *AIAA Journal*, Vol. 15, No. 12, 1977, pp. 1756-1762.

<sup>9</sup>Yule, A. J., AhSeng, C., Felton, P. G., Ungut, A., and Chigier, N. A., "Spray, Drops, Dusts, and Particles, A Study of Vaporizing Fuel Sprays by Laser Techniques," *Combustion and Flame*, Vol. 44, No. 1-3, 1982, pp. 71-84.

<sup>10</sup>Presser, C., Gupta, A. K., and Semerjian, H. G., "Aerodynamic Charac-

teristics of Swirling Spray Flames: Pressure Jet Atomizer," *Combustion and Flame*, Vol. 92, No. 1-2, 1993, pp. 25-44.

<sup>11</sup>Parvez, K., "Studies on Interacting Multiple Burning Liquid Sprays," Ph. D. Dissertation, School of Aerospace and Mechanical Engineering, Univ. of Oklahoma, Norman, OK, April 1995.

<sup>12</sup>Prado, G. P., Lee, M. L., Hites, R. A., Hoult, D. P., and Howard, J. B., "Soot and Hydrocarbon Formation in a Turbulent Diffusion Flame", *Sixteenth Symposium (International) on Combustion*, Combustion Inst., Pittsburgh, PA, 1976, pp. 649-661.

<sup>13</sup>Gupta, A. K., Ramavajjala, M. S., and Chomiak, J., "Burner Geometry Effects on Combustion and NO<sub>x</sub> Emission Characteristics Using a Variable Geometry Swirl Combustor," *Journal of Propulsion and Power*, Vol. 7, No. 4, 1991, pp. 473-478.